

# Thermal behavior of Mullite–Zirconia–Zircon composites. Influence of Zirconia phase transformation

N. M. Rendtorff · L. B. Garrido · E. F. Aglietti

Received: 10 June 2010/Accepted: 30 August 2010/Published online: 29 September 2010  
© Akadémiai Kiadó, Budapest, Hungary 2010

**Abstract** Mullite–Zirconia–Zircon composites have proved to be suitable for high-temperature structural applications, with good mechanical and fracture properties and good thermal shock resistance. In this paper, the special dilatometric behavior of a series of Mullite–Zirconia–Zircon (3–40 vol.%  $\text{ZrO}_2$ ) composites is evaluated and compared with that of a pure Zircon material and explained in terms of the high Zirconia linear thermal expansion coefficient ( $\alpha$ ) and Zirconia martensitic transformation. Linear thermal expansion ( $\alpha$ ) up to 1273 K is studied and correlated with the phase composition of the composites; a linear correlation was found with the m-ZrO<sub>2</sub> content evaluated with the Rietveld method. Zirconia (m-ZrO<sub>2</sub>) dispersed grains containing ceramics material showed a hysteresis in a reversible dilatometric curve (DC). The martensitic transformation temperatures could be evaluated and then compared with the endothermic and exothermic peaks temperatures obtained from the differential thermal analysis (DTA). Furthermore, the hysteresis area was correlated with m-ZrO<sub>2</sub> content, where composites with less

than 10 vol.% ZrO<sub>2</sub> did not show this behavior, and from this content up to 40 vol.% of ZrO<sub>2</sub> a linear increase of the hysteresis area was found.

**Keywords** Ceramic materials · Composite materials · Zirconia · Martensitic transformation · Dilatometry

## Introduction

In many industrial applications, components are required to work in extremely hard conditions, particularly at very high temperatures for long times. For these applications, new ceramic matrix composites have been designed, with both micro and nano-sized reinforcing particles, located at inter or intra-granular positions, this can improve mechanical and thermomechanical performances as well as strongly reduce creep rate. Many attempts are in progress to develop biphasic [1–16] and tri-phasic systems or even tetra-phasic systems [17–25]. Particularly much interest is still being carried out in dispersed zirconia containing ceramic composites with different contents of different types of ZrO<sub>2</sub> grains [1–27].

Zirconia ceramics have attracted great attention to industrial applications in oxygen pumps, sensors, fuel cells, and thermal barrier coatings due to their excellent electrical, thermal, and mechanical properties [26]. Pure Zirconia ceramic exhibits a phase transformation between monoclinic and tetragonal phases. It can be seen that most of the reported m–t and t–m temperatures are in the temperature range 1400–1480 and 1250–1325 K, respectively [27–33].

These transformations temperatures can be evaluated by different methods like differential thermal analysis (DTA), differential scanning calorimetry, high-temperature X-ray

N. M. Rendtorff (✉) · L. B. Garrido · E. F. Aglietti  
Centro de Tecnología de Recursos Minerales y Cerámica  
(CETMIC): (CIC-CONICET-CCT La Plata), Camino Centenario  
y 506, C.C.49, M. B. Gonnet, B1897ZCA Buenos Aires,  
Argentina  
e-mail: rendtorff@cetmic.unlp.edu.ar

N. M. Rendtorff · E. F. Aglietti  
Facultad de Ciencias Exactas, Universidad Nacional de La Plata,  
UNLP, Buenos Aires, Argentina

N. M. Rendtorff  
CIC-PBA, Buenos Aires, Argentina

L. B. Garrido · E. F. Aglietti  
CONICET, Buenos Aires, Argentina

diffraction, neutron diffraction, dilatometry, and Raman scattering. As well as theoretical calculations based in first principles [28, 29].

Over the last decades, considerable advances have been made to improve the fracture toughness of ceramic systems. One of the most important examples is the toughening contribution from stress-induced martensitic transformation of tetragonal grains. Lathabai et al. [2] showed that significant toughening could be obtained by incorporating Zirconia particles ( $\text{ZrO}_2$ ) in a ceramic matrix. Different mechanisms are involved in the toughening of Mullite composite originated by Zirconia additions: stress-induced transformation, microcracking, crack bowing, and crack deflection. In all cases, the operative toughening mechanism depends on such variables as matrix stiffness, Zirconia particle size, chemical composition, temperature, and strength.

Mullite–Zirconia–Zircon composites have proved to be suitable for high-temperature structural applications [18, 24, 25].

Undoubtedly, it is of great technological interest to know the dilatometric behavior of a family of materials for high-temperature applications. It has been stated that the thermal expansion behavior of Zirconia ceramics from a given powder type can be “tailored” within limits by varying the chemical composition and processing variables [34]. This provides some physical property selection capability for engineering applications.

One of the limiting behaviors of several Zirconia containing materials is the thermal shock resistance. This behavior is strongly related to the thermal expansion behavior of the materials [35–38]. Different thermal conditions cause dimensional changes and consequently the magnitudes of the thermal stress are also dissimilar.

Hence it is of technological importance to improve the understanding of this behavior particularly in the Zirconia containing materials which present this special dilatometric behavior.

Recently, other thermal properties were studied in zirconia containing materials, particularly ceramics belonging to the  $\text{ZrO}_2\text{--Y}_2\text{O}_3\text{--TiO}_2$  system. While the thermal conductivity was influenced by the composition the specific heat of the ceramics was unaltered as the  $\text{TiO}_2$  content changed [39]. Other Zirconia containing composites, containing phosphorous oxide combined with hafnium, titanium, and other first row transition metals oxides were synthesized via the flouro complex [40], a thermal analysis evidenced the phase transformation that these composites show at high temperatures.

Regarding to the dilatometric behavior dispersed Zirconia ( $\text{ZrO}_2 = 40$  wt%) grains in a Mullite matrix showed a hysteresis in the reversible dilatometric curve of a Mullite–Zirconia composite [3], and the martensitic transformation temperatures ( $\text{Ms}$ ) could be evaluated. The

**Table 1** Thermal expansion coefficients

	$\alpha/10^{-6} \text{ K}^{-1}$ (300–1273 K)
Mullite	5.3
Zircon	4.5
Zirconia	10.0

thermal expansion hysteresis associated with the monoclinic–tetragonal transformation was also evident in the Mullite–yttria-stabilized  $\text{ZrO}_2$  composite from which the  $\text{Ms}$  temperature could be determined [41]. On the other hand, in a Mullite–Zirconia composite (with 35 wt%  $\text{ZrO}_2$ , and 1.5%  $\text{Y}_2\text{O}_3$ ) a transformation hysteresis was not observed [42]. Perhaps because the monoclinic Zirconia content was not important since the tetragonal phase had been stabilized by the Yttrium oxide. While in the former material [41] the monoclinic was around 80% of the total Zirconia.

The main objective of this work is to study the dilatometric behavior Mullite–Zirconia–Zircon composites and to correlate this behavior to some processing variables especially with phase composition. A second objective is to find the critical  $\text{ZrO}_2$  content composition from which the hysteresis in the dilatometric curve appears for a Zirconia containing composite.

The local thermal expansion mismatch between the constituent phases present in the composite is important, thermal expansion coefficients of these phases are shown in Table 1.

The porosity, mean grain size, and distribution together with the microcracks developed by the martensitic transformation during processing (cooling) and the local thermal expansion mismatch between grains will also influence the dilatometric behavior of the composites.

## Experimental procedure

### Mullite–Zirconia–Zircon composite material

The materials studied in this work were partially characterized, particularly in terms of their thermal shock behavior [24, 25]. Two commercial raw materials were used to obtain the tri-phasic composite: For the first two main phases a commercial powder of Mullite–Zirconia (MZ) (MUZR, ELFUSA LT, Brazil) elaborated from the fusion of raw materials of high purity in electrical arc furnaces was used. The actual chemical composition of this electrofused material is given by the manufacturer ([www.elfusa.com.br](http://www.elfusa.com.br)) and was presented elsewhere [8]. Fusion point: 2123 K; apparent specific mass (NBR8592-1995): 3.71 g/cm<sup>3</sup>; apparent porosity (NBR8592-1995): 3.0%; real density: 3.74 g/cm<sup>3</sup>; reversible linear expansion (1700 K): 0.68%. The <10 µm fraction (obtained by

sedimentation) was milled by attrition to obtain a fine powder (mean diameter,  $D_{50} = 5 \mu\text{m}$ ). This material is composed by Mullite and m-ZrO<sub>2</sub> ( $\geq 40$  wt%) as major crystalline phases.

Zircon, the third principal phase, was introduced by Zirconium silicate (Z) (Mahlwerke Kreutz, Mikron, Germany). With ZrO<sub>2</sub> = 64–65.5 wt%, SiO<sub>2</sub> = 33–34 wt%, Fe<sub>2</sub>O<sub>3</sub>  $\leq 0.10$  wt%, and TiO<sub>2</sub>  $\leq 0.15$  wt% and  $D_{50} = 1.5 \mu\text{m}$ . Specific gravity of 4.6 g/cm<sup>3</sup>, Melting point of around 2473 K and hardness (Mohs) of 7.5.

Composites were prepared from MZ grains and Zircon mixtures containing 15, 45, 55, 65, and 75% (in weight basis) of Zircon and labeled A, B, C, D, and E, respectively, a pure Zircon material was also evaluated and named Z.

Slip cast compacts consisting of prismatic bars of  $7.5 \times 7.5 \times 50 \text{ mm}^3$ . Concentrated 80 wt% suspensions at pH 9.1–9.2 were prepared by adding the powder to aqueous solutions with 0.3% of dispersant (Dolapix CE64, Zschimmers and Schwartz) and NH<sub>4</sub>OH. After mixing, the suspensions were ultrasonicated for 20 min. Probes were sintered at a heating rate of 5 K/min up to 1873 K for 2 h and then cooled to room temperature at 5 K/min.

#### Dilatometric behavior evaluation

The thermal expansion behavior of sintered ceramics from 300 to 1700 K and from 1700 to 700 K was evaluated. The tests were carried out with a high-temperature dilatometer (Netzsch Inc., Germany) using air atmosphere. The final dimension of the sample was approximately  $7.5 \times 7.5 \times 50.0 \text{ mm}^3$ . Data for precise calculation of thermal expansion coefficient were measured in the temperature range 300–1700 K at a heating rate of 10 K/min during heating and cooling.

Experimental thermal expansion coefficients were also compared to a theoretical thermal expansion coefficient ( $\alpha_{\text{theo}}$ ) estimated from the following equation:

$$\alpha_{\text{theo}} = \sum \alpha_i \times V_i \quad (1)$$

where  $\alpha_i$  and  $V_i$  are the corresponding thermal expansion coefficients and volume fraction of each constituent of the composite material.

#### Phase composition

The phase composition was evaluated using the Rietveld refinement of the XRD patterns described elsewhere [25]. The final phase content is shown in Table 2.

**Table 2** Volume composition ( $V_i$ ) of the studied materials

Material	Crystalline phase content (vol.%)		
	Mullite	Zirconia (total)	Zircon
A	61	38	1
B	45	28	27
C	37	20	43
D	29	12	59
E	21	9	70
Z	0	3	97

#### Differential thermal analysis

The differential thermal analyses together with the thermo gravimetric analysis (TG) were carried out simultaneously for the sintered samples in NETZSCH 409/c equipment. They were completed with a 10 K/min heating rate up to 1700 K and were cooled at the same rate down to 700 K. Samples of approximately 550 mg were analyzed in PtRh crucible and dynamic air atmosphere, using pure alumina as reference material.

#### Dilatometric behavior: results and discussions

##### Linear thermal expansion coefficient

As the linear fit of the dilatometric curves of the composites was satisfactory (from room temperature to 1273 K) the experimental linear thermal expansion coefficient  $\alpha_{\text{exp}}$  (300–1273 K) was evaluated from the slope of the linear fitting result of each material. In all cases, the fitting parameters  $R$  were over 0.98.

The true thermal expansion coefficient ( $\alpha_{\text{True}}$ ) was calculated from the differentiated curve of the dilatometric obtained data for a given temperature.

The superposed dilatometric curves of all the materials studied are shown in Fig. 1, the expansion behavior of these materials is stable up to 1273 K. The thermal expansion coefficients of these materials are constant up to 1075 K and a gradual increase with the composition change is observed.

The values of the experimental and theoretical thermal expansion coefficients ( $\alpha_{\text{exp}}$  and  $\alpha_{\text{theo}}$ ) as a function of the Zirconia content (vol.%) of the composites are shown in Fig. 2. As the Zirconia coefficient approximately doubles the Mullite and Zircon values (Table 1), it is expectable that theoretical coefficient increases with the amount of Zirconia. This is clearly shown in Fig. 2, in the same way the qualitative increase is observed for the experimental evaluated coefficients.

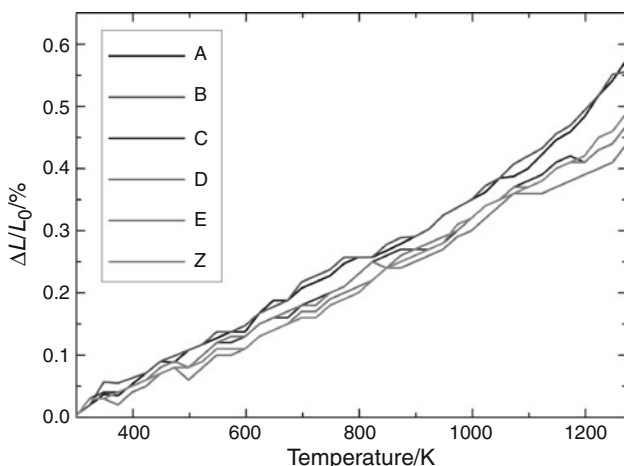


**Fig. 1** Superposed dilatometric curves of the studied materials (from room temperature to 1250 K)

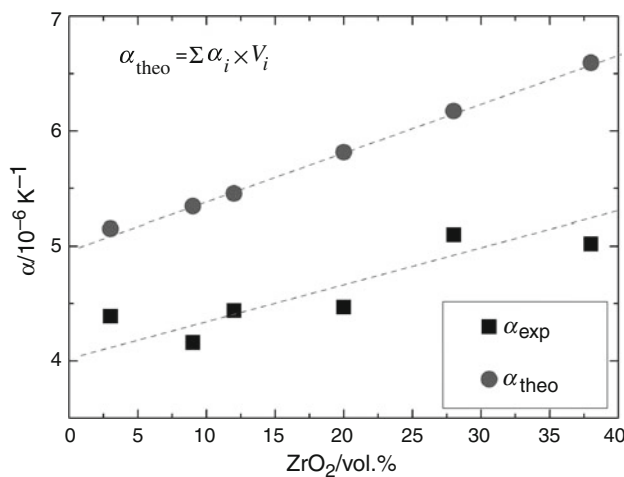


**Fig. 2** Experimental thermal expansion coefficient up to 1250 K ( $\alpha_{\text{exp}}$ ) of the Mullite–Zirconia–Zircon composites as a function of the m– $\text{ZrO}_2$  content (vol.-%)

$$\alpha_{\text{theo}} = \alpha_{\text{mullite}} + V_{\text{zirconia}} (\alpha_{\text{zirconia}} - \alpha_{\text{mullite}}) \quad (2)$$

As the thermal expansion coefficients of Mullite and Zircon do not differ considerably (Table 1) a linear behavior of the theoretical thermal expansion coefficient ( $\alpha_{\text{theo}}$ ) with the Zirconia content in the studied range is expected. This fact is clearly shown in Eq. 2 by expanding Eq. 1 and considering  $\alpha_{\text{Mullite}} \approx \alpha_{\text{Zircon}}$  and that  $1 = V_{\text{Zirconia}} + V_{\text{Zircon}} + V_{\text{Mullite}}$ . Thus the following linear expression for the theoretical thermal expansion coefficient in terms of the volume fraction of monoclinic Zirconia is found.

Linear fit results for  $\alpha_{\text{exp}}$  and  $\alpha_{\text{theo}}$  are represented by Eqs. 3 and 4.

$$\alpha_{\text{exp}} = 4.13 + 0.025 \times V_{\text{zirconia}} \quad (3)$$

$$\alpha_{\text{theo}} = 4.98 + 0.042 \times V_{\text{zirconia}} \quad (4)$$

The fitting  $R$  coefficients were 0.86 and 0.998, respectively, showing that the linear assumption was suitable for the theoretical estimation and was adequately achieved by the experimental evaluation, although the correlation of the  $\alpha_{\text{exp}}$  with the  $\text{ZrO}_2$  content was established.

The difference between the experimental evaluation and the theoretical estimation of the thermal expansion coefficient might be explained by the presence of porosity, the grain size and distribution together with the microcracks developed due to the martensitic transformation. The local thermal expansion mismatch between grains also influences the dilatometric behavior of the composites. All these factors reduced the thermal expansion of the composite and were detected in these composites previously by scanning electron microscopy and mechanical and fracture characterization [25].

The lower value of the experimental slope (Eq. 3) compared to the theoretical slope (Eq. 4) also demonstrates the effect of the Zirconia contents is not only consequence of its higher thermal expansion coefficient.

#### Martensitic transformation in the dilatometric behavior

Solid–solid phase transitions are divided into two broad categories, depending on whether or not long-range atomic migration is involved.

1. Diffusional.
2. Diffusionless.

Diffusionless transformations can be further subdivided into two major categories:

1. Transformations concerning no macroscopic strain.
2. Transformations involving lattice–distortive transformations concerning macroscopic strain of the lattice.

Further, the lattice–distortive transformations having certain crystallographic characteristics are called martensitic transformations.

The two phases involved in a martensitic transformation should have:

1. Lattice correspondence and orientation relationship,
2. Strain invariant plane, and
3. Atom to atom correspondence.

One may choose to further classify martensitic transitions as either “proper” martensitic transformation, where a group–subgroup relationship exists between the symmetry groups of the parent and product phases, or as reconstructive martensitic transitions, where no such group–subgroup relationship exists.

The m–t transformation in  $\text{ZrO}_2$  is believed to be martensitic; however, the details such as the transition path

from the monoclinic to the tetragonal phase or whether the transition is proper are not known [29].

The transformation induces some benefits on the mechanical behaviors of Zirconia containing materials through several mechanisms of toughening (microcracks toughening, transformation toughening, etc.) [26, 27]. It is accompanied by a volume change of approximately 5 vol.%. It consists in shrinkage in the heating cycle and enlargement in the cooling cycle. Besides, the transformation occurs in a range of temperatures depending on the matrix stiffness where the Zirconia particle is embedded [28, 32, 33]. The particle size also influences this transformation. Particles smaller than a critical size do not go through the reverse transformation and remain in a metastable tetragonal form at room temperature. Wang et al. did a complete review on transformation temperatures (m–t and t–m) for zirconia ( $\text{ZrO}_2$ ) [29].

This volume changes can be observed in the dilatometric evaluation of the composites and presents the typical hysteresis form.

This particular instable expansion behavior could be negative for the composite application. Excessive  $\text{ZrO}_2$  content surely affects the thermal shock resistance and strength [24, 25].

In Fig. 3 the complete reversible (300–1700–700 K) dilatometric curves of some Mullite–Zirconia–Zircon composites are shown. In order to achieve a better visualization, the curves were vertically translated. The hysteresis loop is clearly present for A and B composites and it is not observed for the material E and the pure Zircon material (Z).

The temperature at which the transformation occurs was not the same (determined by this method). Both transformations took place at a relatively lower temperature for the composite with smaller Zirconia content. Moreover

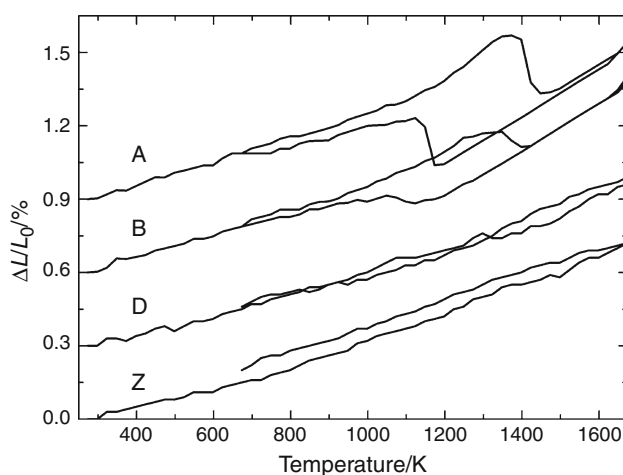


**Fig. 3** Complete dilatometric curve of some Mullite–Zirconia–Zircon composites

materials with higher Zircon content presented a slightly irreversible enlargement.

Besides, the thermal expansion coefficient in a temperature range over the transformation temperature was higher than the lower temperature coefficient, because the slope increased over the loop temperature (Fig. 3).

In Fig. 3, Z sample also presented a little enlargement that begins after the thermal cycle in the pure Zircon material; this was not observed for the composite materials.

#### True alpha

The dilatometric curve (full line) and its respective differential (assumed to be the true expansion coefficient ( $\alpha_{\text{true}}$ )) for the A material are shown in Fig. 4. This was nearly constant up to 1300 K; then an important peak is observed (1400 K), related to the m → t shrinkage. In the cooling cycle a second negative peak is observed around 1150 K that corresponds to the t → m transformation. Both temperatures decreased together with the decrease of zirconia content.

#### Hysteresis loop area

The hysteresis loop area was related with the m- $\text{ZrO}_2$  content quantified by XRD-Rietveld. This was evaluated by the differences in the graphical integration of the heating and cooling curves (between 700 and 1700 K). Finally, the values of the hysteresis loop area for the different composites as a function of the m- $\text{ZrO}_2$  content are shown in Fig. 5. Clearly composite with less than 10 vol.% of m- $\text{ZrO}_2$  did not present the loop, hence the microstructure absorbs the volume changes of the dispersed particles. The loop area of composites containing over 15 vol.% of m- $\text{ZrO}_2$  increased linearly with the Zirconia content. Therefore, the loop area can be used for the

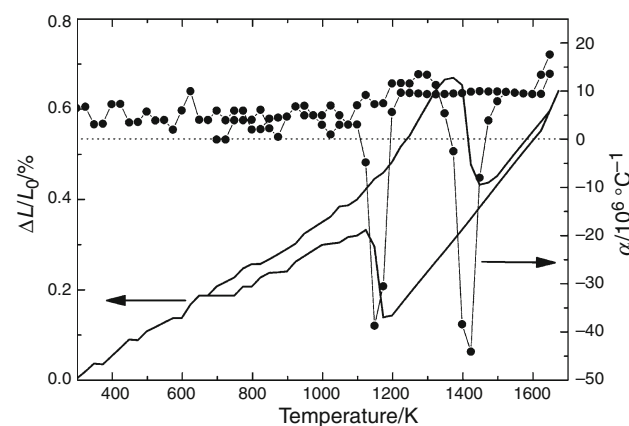


**Fig. 4** Dilatometric and differential dilatometric curves of the A composite

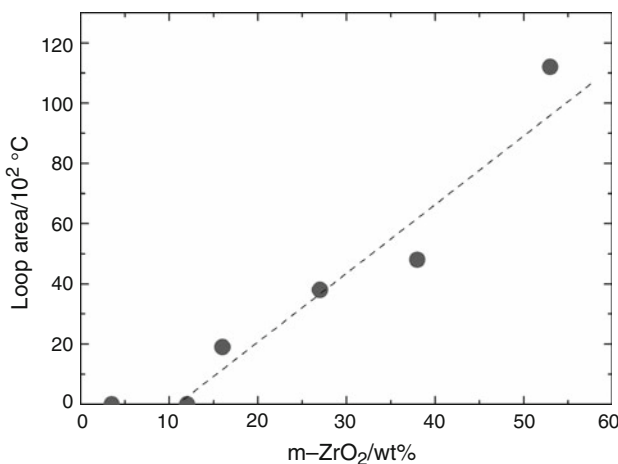


**Fig. 5** Martensitic hysteresis loop area of the dilatometric curves of the Mullite–Zirconia–Zircon composites

estimation of the amount of m-ZrO<sub>2</sub> present in related composites.

#### DTA–TG

The reversible martensitic transformation of Zirconia can be detected by DTA [28]. In the DTA diagrams an endothermic peak, corresponding to the m → t transformation at ≈1400 K during the heating cycle, appeared. Also an exothermic peak at ≈1250–1280 K throughout the cooling cycle appears so, the transformation temperatures can be evaluated. As expected, weight changes from the TG analysis were not significant.

The 1100–1500 K window of the complete DTA (up to 1700 K) for the A, B, C, and E materials is shown in Fig. 6,

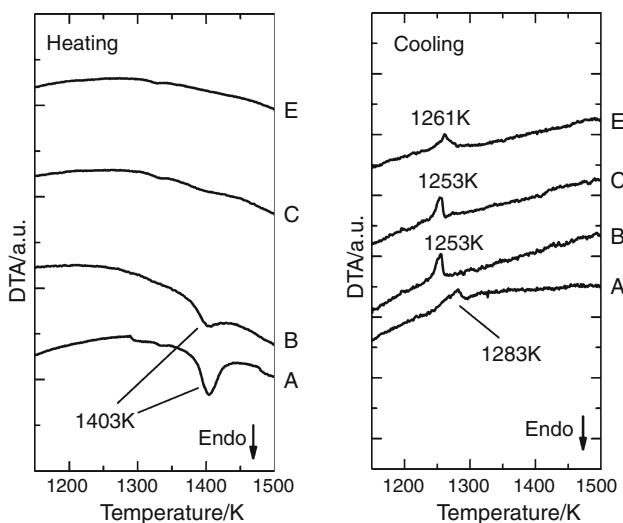


**Fig. 6** Differential thermal analysis (DTA) of A, B, C, and E materials

heating and cooling cycles were separated in order to achieve a better examination.

For the Mullite–Zirconia–Zircon composites A and B with high Zirconia content ( $\geq 25$  vol.%) both peaks were clearly observed at 1400 K; on the other hand for the other materials the m–t endothermic peak is not observed.

The 1250–1280 K exothermic peaks evidenced the tetragonal to monoclinic transformation, which was not detected by the dilatometric analysis. The absence of the first could be explained by the low transformation enthalpy value (5000–6000 J/mol) [28] of the endothermic peak.

Transformation temperatures did not change significantly for the four materials, except for material A (40% of m-ZrO<sub>2</sub> content) in which the t → m exothermic peaks occurred at 30 K above the other materials. As was mentioned the transformation temperatures on heating and cooling are affected by many factors such as particle size, impurities, stress, and thermal history of materials. The literature data reports large discrepancies, and no quantitative analysis has been carried out yet on how these factors can affect the transformation temperatures [27–33].

Monoclinic to tetragonal transformation temperature detected by DTA corresponds satisfactorily with the one detected by dilatometric analysis. But the reverse transformation detected by DTA is more accurate and nearly constant for this family of materials, showing that the nature of the Zirconia grains bonding to the Zircon–Mullite matrix is equivalent.

#### Conclusions

Dilatometric behavior of Mullite–Zirconia–Zircon composite was evaluated in the temperature range where materials exhibits thermal expansions and phase transformation (m–t).

The influence of Zirconia was established. A gradual increase in the thermal linear expansion coefficient with the increase of the zirconia content of the composites was observed below 1250 K. This was lower than a theoretical prediction with a mixing rule, indicating that the effect of ZrO<sub>2</sub> is more complex. Moreover, an indirect evaluation of the microcracks developed during processing was evidenced.

The influence of the martensitic transformation (m–t) in well dispersed Zirconia grains ceramic composite on the thermal expansion behavior was analyzed, an hysteresis loop was observed in the reversible dilatometric curve of composites with enough Zirconia grains ( $\geq 10$  vol.%).

In addition, the loop area can also be used to estimate the monoclinic Zirconia content of these composites because are strongly correlated.

Finally the transformation temperatures was evaluated and correlated with the Zirconia content. The transformation temperatures evaluated by DTA resulted more reliable than the ones detected by the dilatometric analysis.

## References

1. Torrecillas R, Moya JS, De Aza S, Gros H, Fantozzi G. Microstructure and mechanical properties of mullite–zirconia reaction-sintered composites. *Acta Metallurgica* 1993;41(6):1647–52.
2. Lathabai S, Hay DG, Wagner F, Claussen N. Reaction-bonded mullite/zirconia composites. *J Am Ceram Soc*. 1996;79(1):248–56.
3. Hamidouche M, Bouaouadja N, Osmani H, Torrecillas R, Fantozzi G. Thermomechanical behavior of Mullite–Zirconia composite. *J Eur Ceramic Soc*. 1996;16(4):441–5.
4. Jang B-K. Microstructure of nano SiC dispersed  $\text{Al}_2\text{O}_3$ – $\text{ZrO}_2$  composites. *Mater Chem Phys*. 2005;93(2–3):337–41.
5. Hirvonen A, Nowak R, Yamamoto Y, Sekino T, Niihara K. Fabrication, structure, mechanical and thermal properties of zirconia-based ceramic nanocomposites. *J Eur Ceramic Soc*. 2006;26(8):1497–505.
6. Sarkar D, Adak S, Mitra NK. Preparation and characterization of an  $\text{Al}_2\text{O}_3$ – $\text{ZrO}_2$  nanocomposite, Part I: Powder synthesis and transformation behavior during fracture. *Compos Part A Appl Sci Manuf*. 2007;38(1):124–31.
7. Yugeshwaran S, Selvarajan V, Dhanasekaran P, Lusvarghi L. Transferred arc plasma processing of mullite–zirconia composite from natural bauxite and zircon sand. *Vacuum*. 2008;83(2):353–9.
8. Rendtorff N, Garrido L, Aglietti E. Thermal shock behavior of dense Mullite–Zirconia composites obtained by two processing routes. *Ceram Int*. 2008;34(8):2017–24.
9. Belhouchet H, Hamidouche M, Bouaouadja N, Garnier V, Fantozzi G. Elaboration and characterization of mullite–zirconia composites from gibbsite, boehmite and zircon. *Ceramics Silicaty*. 2009;53(3):205–10.
10. Ibarra Castro MN, Almanza Robles JM, Cortes Hernández DA, Escobedo Bocardo JC, Torres Torres J. Development of mullite/zirconia composites from a mixture of aluminum dross and zircon. *Ceram Int*. 2009;35(2):921–4.
11. Mecif A, Soro J, Harabi A, Bonnet JP. Preparation of mullite- and zircon-based ceramics using kaolinite and zirconium oxide: a sintering study. *J Am Ceram Soc*. 2010;93(5):1306–12.
12. Chockalingam S, Traver HK. Microwave sintering of  $\beta$ -SiAlON– $\text{ZrO}_2$  composites. *Mater Des*. 2010;31(8):3641–6.
13. Tür YK, Sünbül AE, Yilmaz H, Duran C. Effect of mullite grains orientation on toughness of mullite/zirconia composites. *Ceram Trans*. 2010;210:273–8.
14. Curran DJ, Fleming TJ, Towler MR, Hampshire S. Mechanical properties of hydroxyapatite–zirconia compacts sintered by two different sintering methods. *J Mater Sci Mater Med*. 2010;21(4):1109–20.
15. Ma W, Wen L, Guan R, Sun X, Li X. Sintering densification, microstructure and transformation behavior of  $\text{Al}_2\text{O}_3$ /ZrO<sub>2</sub>(Y<sub>2</sub>O<sub>3</sub>) composites. 3rd International Conference on Spray Deposition and Melt Atomization (SDMA 2006) and the 6th International Conference on Spray Forming (ICSF VI). *Mater Sci Eng A*. 2008;477(1–2):100–106.
16. Sahnoun F, Saheb N, Chegaar M, Goeuriot P. Microstructure and sintering behavior of mullite–zirconia composites. *Mater Sci Forum*. 2010;638–642:979–84.
17. Calderon-Moreno JM, Yoshimura M.  $\text{Al}_2\text{O}_3$ – $\text{Y}_3\text{AlO}_{12}$ (YAG)– $\text{ZrO}_2$  ternary composite rapidly solidified from the eutectic melt. *J Eur Ceram Soc*. 2005;25(8 Spec. Iss.):1365–8.
18. Hamidouche M, Bouaouadja N, Torrecillas R, Fantozzi G. Thermomechanical behavior of a Zircon–Mullite composite. *Ceram Int*. 2007;33(4):655–62.
19. Naglieri V, Palmero P, Montanaro L. Preparation and characterization of alumina-doped powders for the design of multi-phasic nano-microcomposites. *J Therm Anal Calorim*. 2009;97(1):231–7.
20. Shevchenko AV, Dudnik EV, Ruban AK, Redko VP, Lopato LM. Sintering of self-reinforced ceramics in the  $\text{ZrO}_2$ – $\text{Y}_2\text{O}_3$ – $\text{CeO}_2$ – $\text{Al}_2\text{O}_3$  system. *Powder Metall Metal Ceram*. 2010;49(1–2):42–9.
21. Malek O, Vleugels J, Perez Y, De Baets P, Liu J, Van den Berghe S, Lauwers B. Electrical discharge machining of  $\text{ZrO}_2$  toughened WC composites. *Mater Chem Phys*. 2010;123(1):114–20.
22. Sarkar SK, Lee BT. Evaluation and comparison of the microstructure and mechanical properties of fibrous  $\text{Al}_2\text{O}_3$ -(m-ZrO<sub>2</sub>)/t-ZrO<sub>2</sub> composites after multiple extrusion steps. *Ceram Int*. 2010;36(6):1971–6.
23. Pan C, Zhang L, Zhao Z, Qu Z, Yang Q, Huang X. Changes in microstructures and properties of  $\text{Al}_2\text{O}_3$ /ZrO<sub>2</sub>(Y<sub>2</sub>O<sub>3</sub>) with different content of ZrO<sub>2</sub>. *Adv Mater Res*. 2010;105–106(1):1–4.
24. Rendtorff N, Garrido L, Aglietti E. Mullite–Zirconia–Zircon composites: properties and thermal shock resistance. *Ceram Int*. 2009;35(2):779–86.
25. Rendtorff N, Garrido L, Aglietti E. Zirconia toughening of Mullite–Zirconia–Zircon composites obtained by direct sintering. *Ceram Int*. 2010;36(2):781–8.
26. Zender H, Leistner H, Searle H.  $\text{ZrO}_2$  Materials for applications in the Ceramic Industry. *Interceram*. 1990;39(6):33–6.
27. Kelly P, Rose LF. The martensitic transformation in ceramics—its role in transformation toughening. *Prog Mater Sci*. 2002;47:463–557.
28. Wang C, Zinkevich M, Aldinger F. The Zirconia–Hafnia system: DTA measurements and thermodynamic calculations. *J Am Ceram Soc*. 2006;89(12):3751–8.
29. Luo X, Zhou W, Ushakov SV, Navrotsky A, Demkov AA. Monoclinic to tetragonal transformations in hafnia and zirconia: a combined calorimetric and density functional study. *Phys Rev B Condens Matter Mater Phys*. 2009;80(13):134119.
30. Wang C, Zinkevich M, Aldinger F. On the thermodynamic modeling of the Zr–O system. *Calphad*. 2004;28(3):281–92.
31. Chevalier J, Gremillard L, Virkar AV, Clarke DR. The tetragonal–monoclinic transformation in zirconia: lessons learned and future trends. *J Am Ceram Soc*. 2009;92(9):1901–20.
32. Moriya Y, Navrotsky A. High-temperature calorimetry of zirconia: heat capacity and thermodynamics of the monoclinic–tetragonal phase transition. *J Chem Thermodyn*. 2006;38(3):211–23.
33. Skovgaard M, Ahniyaz A, Sørensen BF, Almdal K, van Lelieveld A. Effect of microscale shear stresses on the martensitic phase transformation of nanocrystalline tetragonal zirconia powders. *J Eur Ceram Soc*. 2010;30:2749–55.
34. Ownby PD, Burt DD, Stewart DV. Experimental study of the thermal expansion of yttria stabilized Zirconia ceramics. *Thermochim Acta*. 1991;190(1):39–42.
35. Kingery WD. Factors affecting thermal stress resistance of ceramic materials. *J Am Ceram Soc*. 1955;38(1):3–15.
36. Hasselman DPH. Elastic energy and surface energy as design criteria of thermal shock. *J Am Ceram Soc*. 1963;46(11):535–40.
37. Hasselman DPH. Unified theory of thermal shock fracture initiation and crack propagation in brittle ceramics. *J Am Ceram Soc*. 1969;52:600–4.

38. Hasselman DPH. Thermal stress resistance parameters of brittle refractory ceramics: a compendium. *Am Ceram Soc Bull.* 1970; 49(12):1033–7.
39. Miyazaki H. The effect of  $TiO_2$  additives on the structural stability and thermal properties of yttria fully-stabilized zirconia. *J Therm Anal Calorim.* 2009;98(2):343–6.
40. Szirtes L, Megyeri J, Kuzmann E. Thermal behaviour of transition- and tetravalent-metal oxides and phosphorous oxide composites. *J Therm Anal Calorim.* 2008;92(2):649–53.
41. Kyaw T, Okamoto Y, Hayashi K. Microstructures and mechanical properties of Mullite-(yttria, magnesia- and ceria-stabilized) Zirconia composites. *J Mater Sci.* 1997;32(20):5497–503.
42. Ruh R, Mazdiyasni KS, Mendiratta M. Mechanical and microstructural characterization of mullite and mullite-SiC-whisker and  $ZrO_2$ -toughened-mullite—SiC-whisker composites. *J Am Ceram Soc.* 1988;71(6):503–12.